Naphthalene-Tagged Copolymer Micelles Based on Polystyrene-*alt*-maleic anhydride-*graft*-poly(ethylene oxide)

Andrew R. Eckert and S. E. Webber*

Department of Chemistry and Biochemistry and Center for Polymer Research, The University of Texas at Austin, Austin, Texas 78712

Received July 21, 1995; Revised Manuscript Received October 26, 1995[⊗]

ABSTRACT: Monoamine-terminated poly(ethylene oxide), PEO-NH_2 (MW ∼ 5000) has been grafted onto a hydrophobic backbone of polystyrene-*alt*-maleic anhydride. The backbone has been tagged with a constant fraction of naphthalene and with varying amounts of PEO-NH_2. Dialysis from dioxane to 100% water produces micelles that have been characterized by light scattering techniques and TEM. The environment of the polymer backbone as a function of the dioxane/water ratio has been characterized by steady state and time-resolved fluorescence techniques. Backbone collapse seems to occur at ∼50% water based on the growth of naphthalene excimer fluorescence. Micelle aggregation numbers appear to vary inversely with the grafting density according to the relation $N_{agg} \sim N_{PEO}^{-3}$, where N_{PEO} is the number of PEO grafts per chain. This relationship can be rationalized by assuming a constant area per PEO coil on the micelle surface.

Introduction

Properties of diblock copolymers as a class of macromolecular architecture continues to be the subject of research for many different applications. Graft copolymers are an important category of block copolymers and offer the potential for some unique features.[1−3] Recent work with graft copolymers includes experimental work from Frere et al.[4] where methoxypoly(ethylene oxide) was grafted onto a poly(acrylic acid) backbone. Tuzar et al.[5] have characterized the effect of selective solvents for both blocks of graft copolymers of polyisoprene-*graft*-polystyrene by light scattering and sedimentation velocity experiments. Watanabe and Matsuda[6] made use of fluorescently tagged polystyrene-*graft*-poly(methyl methacrylate) copolymers to characterize micelle formation. Kim et al.[7] report a unique method of synthesis using a backbone of styrene/maleic anhydride that is grafted onto styrene acrylonitrile rubber. Computer-simulated molecular dynamics of hydrophobic/hydrophilic graft copolymers have been published by Balazs et al.[8] where they report the copolymers behavior as if they were "molecular tweezers" when allowed to interact with a homopolymer of one of the blocks.

Diblock copolymer micelles based on polystyrene and poly(ethylene oxide) have been fairly well characterized.[9,10] Graft copolymers with a hydrophobic backbone and poly(ethylene oxide) as the side chains have only recently received more attention. Early work was reported by Weiss et al. in 1959,[11] but more recent contributions have come from Qui et al.[12] who reported free radical copolymerization of stearyl−poly(ethylene oxide) with styrene as the backbone. Ramasami[13] synthesized a similar graft copolymer with PEO side chains with a molecular weight of 350 and found them to be water soluble and to form micelles. One application of PS−PEO graft copolymers is to serve as supports for solid-phase peptide synthesis, and an extensive review of this topic has recently appeared.[14]

A significant amount of work on these PS−PEO-based water soluble polymers has come from the research groups of Berlinova[15] and Wesslen.[16] Both of these groups have used a variety of synthetic methods while varying the PEO length and grafting density to control certain properties. The former group specifically measured oil and water emulsion properties, thermal properties, and solution properties by means of GPC. They found specifically that the higher the grafting density the longer the elution time for GPC measurements with THF as the solvent.[15c] Wesslen's group also reports a similar finding[16d] in their description of micellizing graft copolymers that are intended for application as biocompatible surfaces.

In this study we report the synthesis of five amphiphilic graft copolymers from starting materials of polystyrene-*alt*-maleic anhyride, PSMA, and monoamine-terminated methoxypoly(ethylene oxide), $CH_3O(CH_2CH_2O)_nCH_2CH_2NH_2$ (referred to as PEO-NH_2 hereafter). The hydrophobicity of the backbone is enhanced by labeling ∼67% of the maleic anhydride active sites with 1-naphthalenemethanamine, Naph-CH_2-NH_2. All five graft copolymers have a specific degree of grafting, and we have characterized them by GPC, NMR, and UV−vis spectroscopy. Upon dialysis to 100% water micelle formation occurred and was characterized by QELS, SLS, TEM, and steady state and time-resolved fluorescence spectroscopy. Evidence suggests the core consists of hydrophobic styrene and naphthalene with PEO dissolved in the aqueous phase as a hydrophilic shell. We find that a higher degree of grafting produces micelles of smaller diameter. This finding can be rationalized as the result of a constant area per PEO coil in the corona of the micelle.

Experimental Section

(a) Synthesis. The backbone for the graft copolymers, styrene/maleic anhydride alternating copolymer, PSMA, was obtained from Scientific Polymer Products, Inc. and has a reported weight average molecular weight of 50 000. This backbone was reacted with a 5000 molecular weight poly(oxyethylene) amine, PEO-NH_2 (Shearwater Polymers), in refluxing dioxane for ca. 14 h. The reaction mixture was allowed to cool to room temperature before 1-naphthalenemethanamine, Naph-Me-NH_2, was added in excess. This solution was then allowed to reflux for 3 h, cooled to its freezing point to accommodate the addition of diazomethane in ether that had been freshly prepared, and stored at 0 °C. Addition of excess diazomethane evolves nitrogen gas and causes the solution to remain yellow for at least 24 h, indicating a high conversion to the methyl ester from existing carboxylic acids.

[⊗] Abstract published in *Advance ACS Abstracts,* December 15, 1995.

0024-9297/96/2229-0560$12.00/0

Chart 1

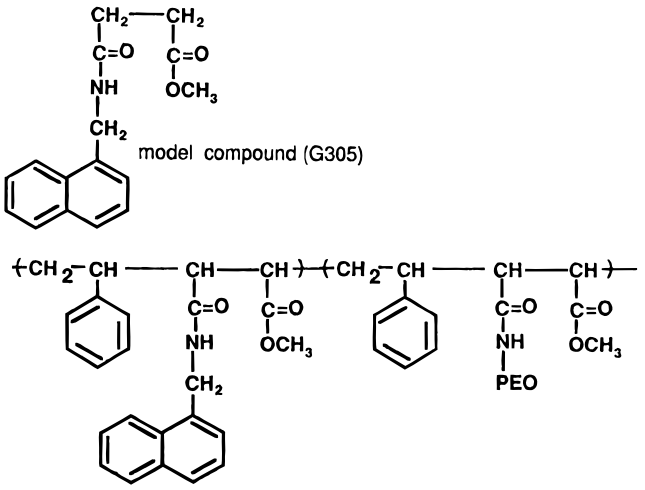

The final structure is represented in Chart 1. Within experimental error we calculate that 67% of all available sites have reacted with the naphthalene derivative, which produces a total molecular weight of ca. 76 000. The ratio of PEO-NH_2 to PSMA was varied to produce five distinct graft copolymers with different degrees of PEO loading (see Table 1). These polymers were purified by extensive dialysis with dioxane, which removes the excess Naph-Me-NH_2, but not the unattached PEO-NH_2. Dialysis with 95% THF/5% water solution removes both, as evidenced by GPC in Figure 1a,b. The dialysis membrane used was Spectra/Por 4 from Spectrum with a nominal molecular weight cutoff of 12 000−14 000.

A model compound for the naphthalene-tagged maleic anhydride backbone monomer unit was synthesized by refluxing Naph-CH_2-NH_2 with a ca. 3 times molar excess of succinic anhydride in dioxane for over 3 h. Diazomethane was added under conditions similar to those mentioned above. Purification produced the expected NMR spectrum. This model compound will be referred to as G305 hereafter.

(b) GPC and UV−Vis Measurements. GPC measurements were performed using four Waters μ Styragel columns (pore sizes 500−10^5 Å); THF was used as the solvent at a flow rate of 1.5 mL/min, with refractive index and UV−vis detectors. Samples were prepared by freeze drying polymer samples from dioxane or THF and were easily redissolved in THF. The GPC traces depended on the relative PEO content of the graft copolymers as well as the precise method of purification using different dialyzing solvents. Measurements of the percentage of active sites on the backbone tagged by naphthalene and the degrees of branching by PEO were determined by UV−vis spectra. The extinction coefficient for the substituted naphthalene attached to the backbone, $\epsilon = 6230$ cm^{-1} M^{-1}, at 284 nm in dioxane, was estimated using the model compound G305. This is very close to the extinction coefficient for 1-methylnaphthalene ($\epsilon = 6390$ cm^{-1} M^{-1} at 281 nm).[17] In order to estimate the number of PEO grafts precise solutions of the graft copolymers in spectral grade dioxane were prepared for UV absorption, as will be discussed later.

(c) NMR. Purified graft copolymers were dissolved in deuterated chloroform for proton NMR spectroscopy (performed at 500 MHz on a GE 6N-500). Integrated spectra were used to calculate the ratio of aromatic protons to the aliphatic protons of PEO. Aromatic protons due to styrene and naphthalene extensively overlap in the range between 6.0 and 8.2 ppm, compared to the peak for PEO protons at 3.6 ppm. From the percentage of naphthalenes attached to the backbone obtained from UV−vis spectroscopy combined with the integrated NMR results, we calculate the number of PEO chains per backbone given in Table 1 under the NMR column.

(d) Micelle Preparation. Micelle solutions were prepared by stepwise dialysis from 100% dioxane to 100% 0.02 M aqueous NaCl. Solutions were filtered using 0.45 μm Acrodisc filters before QELS measurements.

(e) Light Scattering. Quasi-elastic light scattering, QELS, was performed to determine the hydrodynamic diameters of graft copolymer micelles. The scattered emission of a polarized HeNe laser ($\lambda = 632.8$ nm) is measured at $\theta = 90°$ and collected on a Brookhaven BI 2030 correlator. All measurements were taken at 25 °C with the viscosity, η, and index of refraction, n, assumed to be that of pure water for the dilute solutions used in this work. The decay rate of the scattering correlation function, Γ, is obtained from the slope of the log of the scattering correlation function and is defined by[18]

$$\Gamma = Dq^2 \tag{1}$$

where D is the diffusion coefficient and q is the scattering vector

$$q = (4\pi n/\lambda)\sin(\theta/2) \tag{2}$$

The Stokes−Einstein relationship, eq 3, is used to calculate the hydrodynamic diameter (d_h).

$$d_h = (kT/3\pi\eta D) \tag{3}$$

The polydispersity (pd in Table 2) is given by the ratio μ_2/Γ, where μ_2 is the second cumulant of the decay function.

Static light scattering measurements were performed and analyzed in the laboratory of Prof. Petr Munk. Refractive index increments, dn/dc, were estimated from standard values for PEO and PS latexes in water.[19] Three dilute concentrations of each polymer sample were measured as a function of scattering angle to create Zimm plots that were extrapolated to zero concentration to obtain the molecular weight of the micelle. The concentration of the solutions used were determined by the optical density at 286 nm from the naphthalene and knowledge of the composition of the polymer.

(f) Transmission Electron Microscopy (TEM). TEM measurements were performed by John Mendenhahl at The Cell Research Institute at the University of Texas at Austin. Samples were prepared by freeze drying a dilute solution of micelles (<0.01 g/L) on a thin layer of graphite layered over a copper grid and then stained with RuO_4. A distribution analysis of the micelles in the photographs was performed, and the results are presented in Figure 2 and Table 2.

(g) Fluorescence Spectroscopy. Steady state fluorescence spectra were taken on a Spex Fluorolog fluorometer with double monochromators for both the excitation and emission radiation. The data were then collected and stored on a personal computer using DM3000 software from Spex. Steady state fluorescence quenching data were analyzed according to the adapted Stern−Volmer equation for a two-state model:[20]

$$\frac{I_o}{I_o - I} = \frac{1}{f_a} + \frac{1}{K_{SV} f_a [Q]} \tag{4}$$

In this equation I_o is the intensity of fluorescence in the absence of quencher, I is the intensity when quencher is present at a concentration [Q], f_a is the fraction of chromophores accessible to the quencher, and K_{SV} is the Stern−Volmer quenching constant for the exposed chromophores.

Time-resolved fluorescence decays were measured using the method of time-correlated single photon counting. A mode-locked Nd:YAG laser is frequency doubled and serves to pump a cavity dumped dye laser that is circulating Rhodamine 6G. This radiation is then frequency doubled by a KDP crystal to produce an excitation wavelength of ∼293 nm. The signal is measured at a right angle, with polarizers set at the magic angle (54.7°), and focused through a monochromator to a microchannel plate detector. Further details of this system can be found elsewhere.[18]

The observed decay is a convolution of the sample decay and the response function of the laser pulse. The sample decay is conveniently fit as a multiexponential decay function

$$I(t) = \sum_i \alpha_i \exp(-t/\tau_i) \tag{5}$$

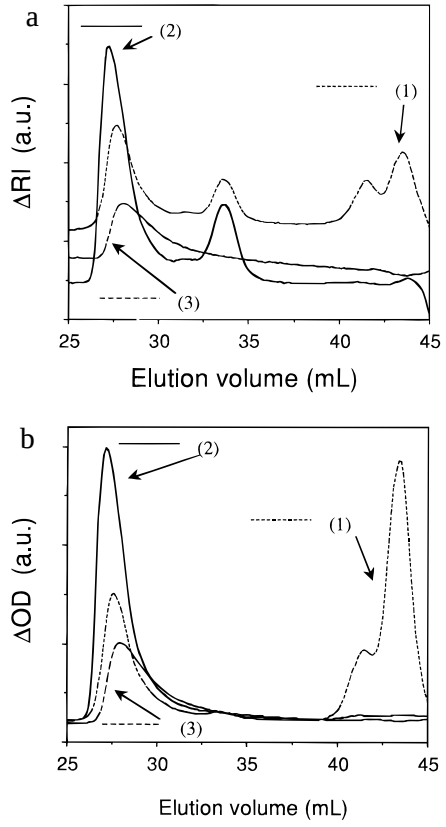

Figure 1. (a). Gel permeation chromatography results as detected by refractive index for G125 at different methods of purification. (1) is the unpurified reaction product, (2) is purified by dialysis with dioxane, and (3) is purified by dialysis with a 95% THF/water solution. (b). Same notation of sample as in Figure 1 except with UV−vis detection.

using a nonlinear least-squares curve-fitting approach using the Levenberg−Marquardt algorithm.[20,21] In this process one to a maximum of five exponentials with varying preexponential factors and lifetimes are adjusted in successive iterations. This process continues until the best fit is obtained between the calculated and actual decay curves. The best fit is determined by reaching a minimum value for the weighted residuals squared (χ^2) and is further evaluated with respect to the randomness of the residuals and autocorrelation function. The average lifetime quoted later is calculated using the lifetimes and pre-exponential factors calculated with the following formula.

$$\langle\tau\rangle = \sum_i \alpha_i\tau_i / \sum_i \alpha_i \qquad (6)$$

Results

(a) Compositional Characterization. Parts a and b of Figure 1 compare GPC traces using refractive index and UV absorption detection, for sample G125 at different levels of purification: (1) unpurified reaction product, (2) purification by dialysis with dioxane, and (3) purified by 95% THF:5% water dialysis. It is evident that excess $NaphMeNH_2$ is removed by either dialysis method but removal of excess PEO-NH_2 requires the THF:water mixed solvent.

In Table 1 is presented the percentage of maleic anhydride groups that have $NaphMeNH_2$ attached. These values were determined by UV−vis measurements of precisely prepared solutions of the graft copolymers that had been dialyzed only with dioxane to remove unattached $NaphMeNH_2$. The mass of the attached $NaphMeNH_2$ is subtracted from the total mass of the sample. The ratio of PEO/PSMA is known from

Table 1. Graft Copolymer Composition and Molecular Weight (MW) As Determined by UV−Vis and NMR Measurements

		N_{PEO}[b]		% yield[c]		MW (10^{-4})[d]		
polymer	N_{PEO} (mix)[a]	UV−vis	NMR	UV−vis	NMR	UV−vis	NMR	% Napth[e]
G125	20	5.9	10.7	30	53.5	10.6	13.0	66.3
G105	10	4.2	5.9	42	59.0	9.70	10.6	65.3
G175	7.5	2.6	5.0	34	66.7	8.90	10.1	67.7
G155	5	2.1	3.4	42	68.0	8.65	9.3	67.8
G195	2.5	1.1	1.8	43	72.0	8.15	8.5	68.6
av				38	63.9			67.1 ± 1.3

[a] The number of PEO branches per graft backbone based on the reaction mixture. [b] The number of PEO branches per polymer as determined by UV−vis spectroscopy and NMR. [c] Percent yield of grafting reaction by UV−vis is spectroscopy and NMR. [d] Molecular weight based on a ~76 000 backbone and the number of grafts per chain. [e] % Naph signifies the percent of maleic anhydride sites on the backbone with 1-naphthalenemethanamine attached.

the starting mass ratio of the reactants, so we can calculate the mass of PEO and PSMA in the sample. From simple stoichiometry we can calculate the percentage of maleic anhydride sites in the alternating PSMA that are tagged by naphthalene. The reproducibility of the tagging percent for all five samples is excellent with an average value of 67.1% (±1.3%).

Purification by dialysis with 95% THF:5% water solutions removes both the excess $NaphMeNH_2$ and PEO, as evidenced by trace 3 in Figure 1a,b. UV−vis measurements of all five samples purified by dialysis with this THF:H_2O mixture allow us to calculate the mass of attached $NaphMeNH_2$, from which we can determine the mass of PSMA using the percent tagging values discussed above. All remaining mass is attributed to attached PEO, and these results are presented as the number of PEO species per chain (N_{PEO}) in Table 1 under the UV−vis column. The error in the extinction coefficient is estimated to be ±8%. Gravimetric error is also a source of uncertainty in the values quoted here, given that the total mass of the polymer samples was on the order of a few milligrams.

A complementary analysis of the PEO grafts per backbone was obtained through NMR analysis, as was discussed in the Experimental Section. The results in Table 1 (NMR column) display the same trend in the degree of grafting obtained as described above although the N_{PEO} values are an average of 1.7 times greater than the values obtained from the UV−vis measurements. There are at least two explanations for the discrepancy in these two sets of results: (1) The NMR signal intensity may be biased to favor lower molecular weight species with longer relaxation times which may have a degree of grafting that differs from the true average. However, high-temperature NMR experiments in deuterated DMSO produced the same result as the room temperature experiment, suggesting that this bias is not present. (2) The extinction coefficient we are assuming for the substituted naphthalene is too low, which produces an overestimate of PSMA mass and hence an underestimate of the mass of PEO. This latter method is very dependent on effective separations and gravimetric accuracy, such that we favor the NMR result for N_{PEO}.

The yield data obtained from the NMR data demonstrate a higher yield as the concentration of PEO is decreased in the starting reaction mixture (Table 1). It is reasonable to suppose that as the grafting density increases, steric access to the reaction sites decreases.

Table 2. Size Analysis of Graft Copolymer Micelles

micelle	d_h[a] (pd)/nm	d_{TEM}[b]/nm	MW_{SLS}[c] (±sd) $\times 10^{-6}$	N_{agg}[d] UV−vis	N_{agg}[d] NMR	N_{agg}(QELS)[e]	N_{agg}(TEM)[e]
G125	28 ± 1 (0.07)	16.2 ± 2.6	2.09 (±0.12)	20	16	24	18
G105	34 ± 2.5 (0.10)	19.8 ± 2.8	5.75 (±0.14)	59	55	57	32
G175	46 ± 4.4 (0.19)	23.9 ± 3.6	6.967 (±0.13)	78	69	190	57
G155	68 ± 11.2 (0.13)	30.6 ± 3.9	40.9 (±0.86)	473	440	822	119
G195	94 ± 5.9 (0.10)	52.5 ± 13.3	202 (±4.0)	2480	2370	2430	600

[a] d_h is the hydrodynamic diameter obtained from QELS measurements where pd stands for polydispersity from QELS measurements. [b] d_{TEM} is the average diameter obtained from the TEM distribution functions in Figure 2. [c] Molecular weight obtained by static light scattering (sd = standard deviation of molecular weights). [d] This aggregation number is based on SLS. The difference in the aggregation numbers arises from the different estimates of the number of PEO grafts on the chain. [e] Based on d_h (from QELS) or d_{TEM} (see text). These values do not depend on N_{PEO} because they are based on the density of the polystyrene core.

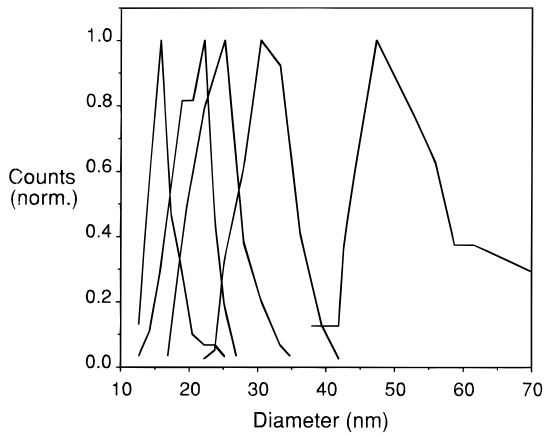

Figure 2. Analysis of micelle diameters obtained from TEM to produce a distribution of sizes for each graft copolymer micelle sample. From left to right the sample number and average number of PEO molecules per chain (based on NMR, see Table 2) are G125 (10.7), G105 (5.9), G105 (5.0), G155 (3.4), and G195 (1.8).

Although the UV−vis measurements were less precise, these data confirm the trend from smaller to higher grafting densities. Note that the yields calculated from the UV−vis measurements were essentially constant. A Poisson distribution was used to analyze the distribution of the number of branches per chain using the average number from the NMR data in Table 1. According to this distribution analysis all samples, except for G195, have less than 4% of PSMA that remains untagged. These results were calculated using 50 000 for PSMA and 5000 for PEO as the number average molecular weights for the sake of convenience.

(b) Size Analysis of Graft Copolymer Micelles. Table 2 presents data from QELS, TEM, and SLS of graft copolymer micelles dialyzed to 100% water. All three techniques verify that the polymers with the highest degree of grafting form micelles with the smallest diameters. QELS values of d_h in Table 2 are the average from several different dialysis preparations, which is the source of the cited standard deviation. The average polydispersities that we measured were relatively high compared to the very monodisperse micelles formed from diblock copolymers that typically fall in the range 0.04−0.09.[18a]

Figure 2 is the distribution analysis carried out on the TEM photographs. From this distribution we calculate a number average diameter (d_{TEM}) and standard deviation that are presented in Table 2. It is our experience that TEM typically produces smaller diameters than light scattering. There are two factors that contribute to this phenomena: (1) Light scattering is weighted in favor of larger objects (i.e. it is a *z*-average). (2) Freeze-dried micelles may undergo a change in volume because the shell structure of the PEO chains is likely to collapse when no longer solvated. The "weight average diameter" compared to the number average proved to be less than 10% higher, suggesting a low polydispersity.[22]

Static light scattering measurements were used to obtain the molecular weights of the micelles from Zimm plots of the data from three or more concentrations (Table 2). The uncertainty in the molecular weights of the micelles was obtained from a standard analysis of the uncertainty of the *y*-axis intercept from the average error between the best fit and the experimental data in the Zimm plots. The trend in molecular weight is consistent with the graft copolymer micelle diameters. Dividing by the appropriate molecular weight of the unimer (the PEO contribution is different according to the UV−vis and NMR estimate of N_{PEO}) yields the aggregation number (N_{agg}) of the micelle presented in Table 2. This is direct evidence that the micelles are multiunimeric rather than single unimer micelles.

(c) Photophysics of Graft Copolymer Micelles. The naphthalene chromophore is very sensitive to its environment and has a strong tendency to form excimers, especially in water.[23,24] The photophysics reflect the change in polymer configuration that occurs by varying the composition of the dioxane/water mixed solvent. Figure 3a illustrates this for the steady state fluorescence spectra for G125 as a function of dioxane/water. For pure dioxane the graft copolymers have strong monomeric emission at 340 nm with only a slight excimer shoulder at 400 nm. As the fraction of water increases, the excimer component begins to dominate the spectra. The near-isobestic point at approximately 360 nm in Figure 3a indicates the presence of only two fluorescent species, monomer and excimer. In Figure 3b we plot the monomer to excimer ratio (the area for monomer and excimer emission is taken to be 330−350 nm and 390−410 nm, respectively). The monomer to excimer ratio decreases dramatically until the water content reaches 30% and decreases more gradually thereafter. This trend is similar for all graft copolymer micelles and we infer that the environment of the backbone in mixed solvents does not vary with the number of grafts. Figure 4 presents the change in light scattering intensity as a function of water content. The dramatic change in scattering intensity indicates that these graft copolymers aggregate at around 50% water. Combining these complementary results suggests that the backbone first collapses with the addition of ca. 30% water to produce excimer fluorescence and then these collapsed polymers form micelles as the water content increases.

One also obtains insight into the behavior of the PSMA/Naph backbone as a function of solvent from the time-resolved fluorescence decays for both monomer and

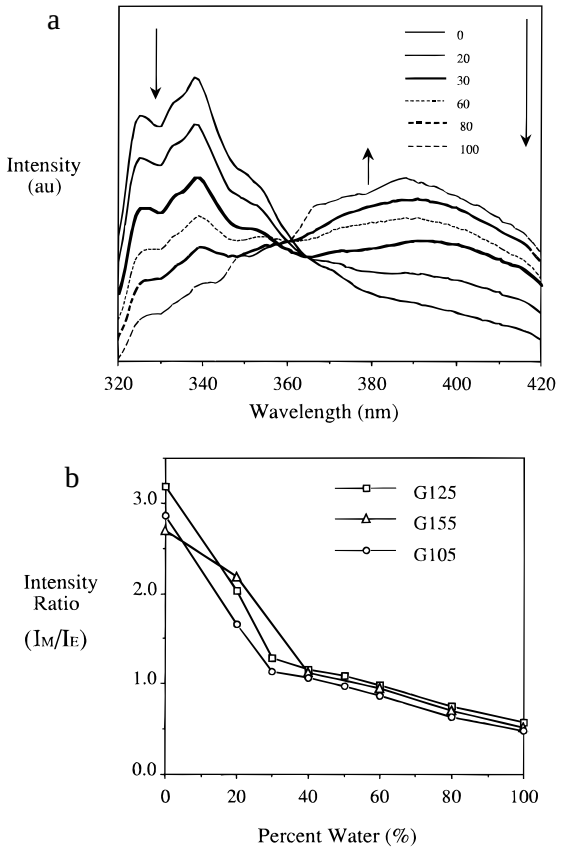

Figure 3. (a). Steady state fluorescence spectra of G125 graft copolymer micelles as a function of percentage water in dioxane solutions. (b). Monomer to excimer emission intensity ratio as a function of the percentage water in dioxane solutions for three graft copolymer micelles. Data from the steady state spectra, (a), are analyzed by calculating the monomer intensity from 330 to 350 nm and dividing by the excimer intensity from 390 to 410 nm.

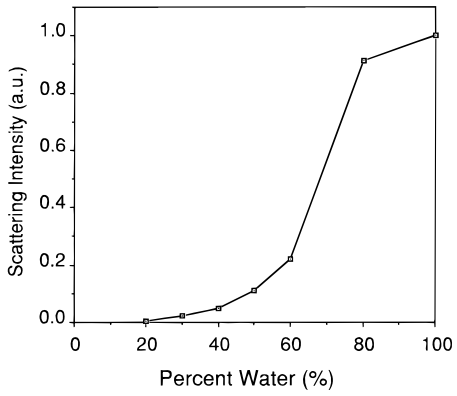

Figure 4. Scattering intensity as measured by QELS for G105 micelles as a function of percentage water in dioxane solutions.

excimer emission (measured at 340 and 410 nm, respectively; see Figure 5 for a typical pair of decay curves). It is interesting that there is a significant rise time for excimer formation at all solvent compositions. The rise time can be attributed to two phenomena that contribute to the excimer emission: (1) segmental diffusion or rotation during the naphthalene singlet excited state lifetime to a position of cofacial overlap with a neighbor naphthalene, which favors excimer formation; (2) energy migration (presumably through the Förster mechanism) to preformed excimer sites.[25] The relatively long rise times at low concentrations of water are reasonably assigned to segmental motion. At

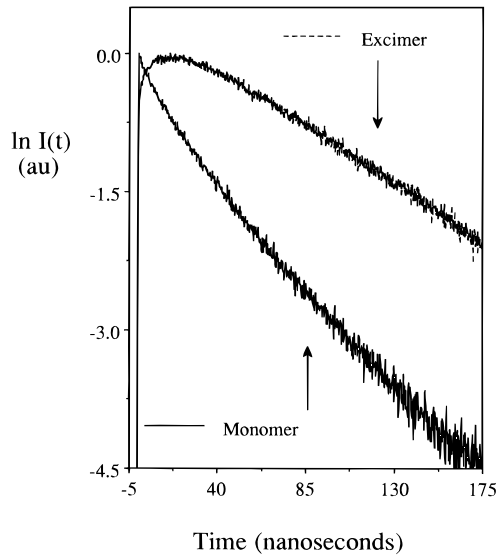

Figure 5. Time-resolved fluorescence decays of G125 in a 40% water in dioxane solution. The monomer and excimer decays are measured at 340 and 410 nm, respectively.

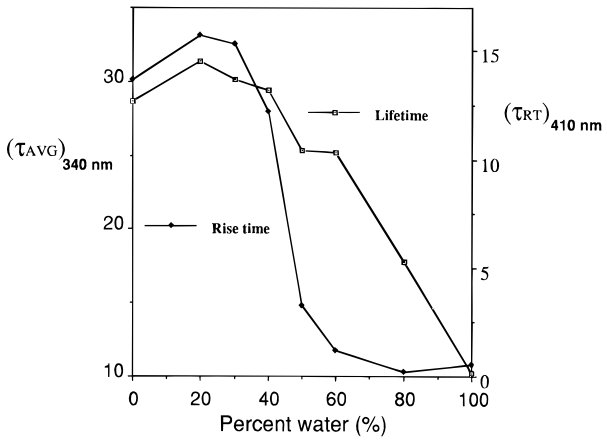

Figure 6. Average lifetime for the monomer (at 340 nm) and rise time for the excimer (at 410 nm) for G125 graft copolymer micelles as a function of percentage water in dioxane/water solutions.

higher concentrations of water it seems reasonable to expect that the naphthalenes are collapsed into close contact, maximizing the probability for Förster energy transfer.[26] Finally, at 100% water the naphthalene moieties are locked into the glassy micelle core where segmental motion is limited,[25] and energy migration to an excimer-forming site or direct excitation of an excimer is likely. Energy transfer/migration can occur on a much faster time scale than segmental motion, consistent with the shorter rise times observed.[27] The rise time is plotted as a function of solvent composition in Figure 6. The multiexponential fitting parameters for the excimer decay as a function of H_2O content are in Table 3.

For the monomer emission at 340 nm we observe similar increases in the decay rates with increasing H_2O content (see the solvent dependence of $\langle\tau\rangle_{340}$, eq 6, in Figure 6). The fluorescence decays for the monomer emission had to be fit to multiexponential decays for all solvent compositions, which indicates an ensemble of varying environments for the naphthalene chromophores (fitting parameters not given). Similar trends in time-resolved fluorescence were found for G105 and G155. It is also noteworthy that the average fluores-

Table 3. Excimer Emission, $\lambda = 410$ nm[a]

% H_2O	τ_1	α_1	τ_2	α_2	τ_3	α_3	τ_4	α_4	$\langle\tau_{av}\rangle^b$	$\tau_{decay}{}^c$	χ^2
0	5.18	−0.64	17.6	−1.32	44.1	2.97			104	44.1	1.02
20	5.12	−0.67	19.0	−1.99	55.7	3.66			163	55.7	1.02
30	0.69	−0.28	7.30	−0.93	21.45	−1.90	64.1	4.12	216	64.1	1.01
40	1.90	−0.55	15.9	−1.55	71.4	3.09			196	71.4	1.05
50	0.46	−0.63	6.63	−0.51	51.8	0.26	72.0	1.88	145	69.5	1.00
60	1.23	−0.63	65.2	−0.08	66.6	1.71			108	66.6	1.13
80	0.39	−0.51	21.8	0.74	70.1	0.77			70.2	46.5	1.04
100	0.56	−1.03	18.3	0.95	40.9	0.46	74.6	.62	81.6	40.5	1.06

[a] Fit to eq 5, τ_i in ns. [b] $\langle\tau_{av}\rangle = \sum_i \alpha_i\tau_i/\sum_i\alpha_i$. [c] Same as in footnote *a* except with only the positive preexponential factors.

Table 4. Area per Emerging PEO Coil for Micelles[a]

	S_{PEO} (QELS)		S_{PEO} (SLS)		S_{PEO} (TEM)	
micelle	UV−vis	NMR	UV−vis	NMR	UV−vis	NMR
G125	713	393	762	450	792	437
G105	755	537	743	544	910	648
G175	814	423	1094	593	1220	634
G155	619	382	743	471	1180	728
G195	823	503	817	507	1310	801
av	745 ± 83	488 ± 69	832 ± 150	513 ± 58	1080 ± 221	650 ± 137

[a] In each case the average number of grafts per polymer is taken from UV−vis or NMR data. The diameter of the core is taken from the aggregation number calculated for QELS, SLS, or TEM, respectively.

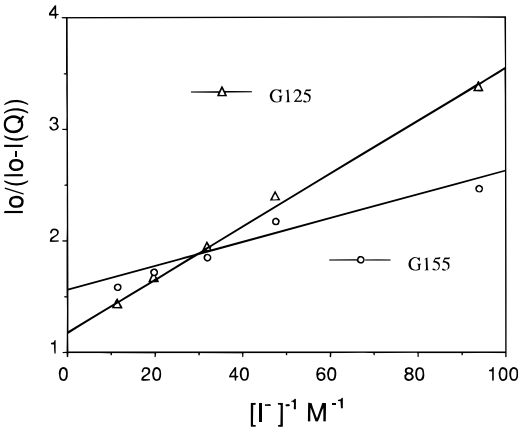

Figure 7. Fluorescence quenching of graft copolymer micelles of G125 and G155 plotted according to eq 4 of the text, with KI as quencher.

cence lifetime for naphthalene in 100% dioxane of 28.7 ns agrees with our model compound G305.

Another method of probing the graft copolymer micelle and water interface is by fluorescence quenching with I^- (note that it is primarily the excimer that is quenched under these conditions. Figure 7 compares steady state fluorescence quenching for G155 and G125 by way of a modified Stern−Volmer plot appropriate for a two-state model of quenching (see eq 4).[20] The overall quenching efficiency is similar to that observed in our previous studies of a chromophore in a protected environment.[28] From the *y*-intercept we calculate the fraction accessible to quencher, f_a, to be 84% and 66% and a quenching rate constant from the inverse of the slope to be 51 and 142 M^{-1} for G125 and G155, respectively. These values agree with the expectation that for the smaller micelle there will be a higher surface area to volume ratio, with a higher fraction of naphthalenes accessible to the aqueous phase.

Discussion

QELS, TEM, and SLS data all demonstrate the same relative trend in size, and we propose a theoretical analysis of the factors that determine the size of the micelle later in this section. In our previous study of the adsorption of hydrophobically end-tagged PEO onto a polystyrene latex particle we found that there was an average area per PEO of ∼260 Å^2.[28] For the present system we can also compare the area per PEO at the core−shell interface. Each technique yields slightly different values for the aggregation numbers, N_{agg}, and hence the area per PEO coil, S_{PEO}.

(1) QELS. In our previous work on the maximum adsorption of PEO on PS latexes the hydrodynamic diameter increased by ∼10 nm.[28] Using this as our model for the shell thickness, we can estimate a core diameter, based on the d_h values (see Table 2). We assume a core density of 1.05 g/cm^3,[29] which is the value used for prior calculations, to obtain the core mass, and dividing by the molecular weight of the backbone, ∼76 000, produces the aggregation number (see Table 2). The aggregation number multiplied by the number of PEO per backbone gives the total number of PEO in the micelle. Dividing the total surface area by the total number of PEO gives the area per PEO.

(2) SLS. The total mass of the micelle is directly obtained from the SLS measurement and was used to calculate the aggregation number (Table 2) and thereby the mass of the core, from which the volume and surface area of the core proceeded as described above.

(3) TEM. For TEM the average diameter was used as the core diameter from which N_{agg} is obtained, like the QELS calculation. A calculation like that for the QELS data was carried out to determine S_{PEO}.

Table 4 contains the S_{PEO} values obtained by using the grafting densities from the UV−vis or NMR results (recall that the latter grafting densities are higher than the former by a factor of 1.7). The value of S_{PEO} based on averaging the QELS and SLS are ∼790 and ∼500 Å^2 for the UV−vis and NMR N_{PEO} values, respectively. We believe the SLS and NMR results to be the most accurate estimate of S_{PEO}. The values in Table 4 tend to be one-half to one-third of the area per PEO at which coil overlap begins to occur, as calculated from the root mean square end to end distance of 1570 Å^2. The area per polymer found in our previous work was ∼260 Å^2 for end-adsorbing polymers that were strongly overlapping.[28] The larger S_{PEO} values obtained for these micelles may reflect the effect of the relatively hindered main chain.

Diameters derived from TEM measurements are smaller and therefore yield smaller aggregation numbers and larger S_{PEO} values. The standard deviation (±20%) of the TEM average is the highest of the three measurements. The most consistent results are for the smallest and most monodisperse sample, G125, which has an average area per PEO of 756 Å^2 for UV−vis and 427 Å^2 for NMR.

While the polymer from which the graft polymers discussed herein is a typically polydispese polymer derived from a free-radical polymerization ($M_w/M_n \approx 1.5$), the micelles derived from the graft polymers are reasonably monodisperse. This suggests that when amphiphilic polymers self-assemble into micelles, or other organized structures, they incorporate different molecular weight polymers, as required to achieve the most stable shape and density of surface amphiphiles. This is similar to the statistics encountered in "living polymerizations", since there is no termination step.[30] Based on the theory of colloidal stabilization, it is reasonable to assume that an important stability criterion is an optimal area for each PEO chain that extends into the aqueous phase.[31] In the star model of micelle formation from diblock polymers due to Halperin,[32] the core radius scales according to $R_c \propto N_B^{3/5}$ (N_B is the degree of polymerization of the core block) and the aggregation number scales according to $N_{agg} \propto N_B^{4/3}$, so the area per emerging chain of the corona (designated as polymer A) is given by $S_A \propto R_c^2/N_{agg} = N_B^{-2/15}$. Therefore for a star micelle with constant N_B the area per emerging chain is also predicted to be constant.[33]

This criterion suggests the following simple relations. The area per PEO chain is given by

$$S_{PEO} = \frac{4\pi R_c^{\,2}}{N_{PEO} N_{agg}} \tag{7}$$

where R_c is the radius of the micelle core, N_{PEO} is the number of PEO grafts per chain, and N_{agg} is the aggregation number of the micelle. It will be assumed that S_{PEO} is a constant based on former work with PEO.[28] The aggregation number of the micelle is also related to the radius of the micelle if we assume that the density of the micelle core is constant:

$$\frac{4\pi}{3}\frac{R_c^{\,3}\rho_{core}N_0}{N_{agg}} = M_{core} \tag{8}$$

where ρ_{core} is the density of the core, N_0 is Avogadro's number, and M_{core} is the molecular weight of the polymer that makes up the core (note that the contribution of the PEO to the graft polymer molecular weight is ignored because this polymer is outside the core). Solving for R_c and substituting into eq 7 yield

$$N_{agg} = \left[4\pi\left(\frac{3M_{core}}{\rho_{core}N_0}\right)^2\frac{1}{S_{PEO}^{\,3}}\right]\frac{1}{N_{PEO}^{\,3}} \tag{9}$$

This inverse relationship between N_{agg} and N_{PEO} works reasonably well, as illustrated in Figure 8 using the data in Tables 1 and 2 for SLS and NMR techniques.[34] Although the different methods of determining N_{agg} (SLS, QELS, and TEM) and N_{PEO} (UV−vis and NMR) do not agree perfectly, as noted before, the N_{PEO} values are proportional to each other (see Table 1), the relationship in eq 9 will not be changed. The numerical

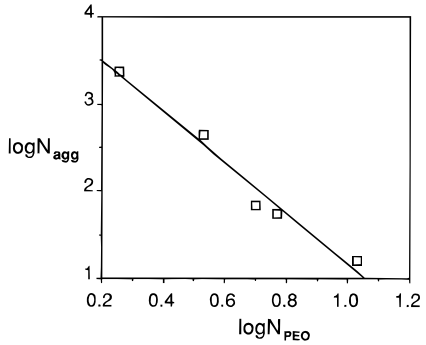

Figure 8. Logarithmic plot of the aggregation number, N_{agg}, versus grafting density, N_{PEO}.

value for the constant in eq 9 is ca. 1.44×10^4 for $M_{core} = 7.6 \times 10^4$, $\rho_{core} \sim 1$ g/cm^3, and $S_{PEO} \sim 500$ Å^2, which agrees remarkably well with the intercept in Figure 8 ($\log(1.44 \times 10^4) = 4.16$, compared with 4.08). Such excellent agreement is undoubtedly fortuitous but supports the reasonableness of the model. It would be of considerable interest to extend these concepts to backbone polymers of different molecular weights and hydrophobicities and similarly to change the properties of the hydrophilic graft. From a practical point of view it is certainly easier to carry out graft modification of a linear polymer in order to modify micelle formation and properties than to prepare diblock or triblock copolymers using anionic polymerization methods.

Our knowledge of the core of these micelles is sketchy and is inferred from the photophysical studies of the naphthalene. There is a smooth conversion from primarily monomer fluorescence to primarily excimer fluorescence as micelles are formed, as expected. Although the naphthalene might be expected to be close to the core−aqueous interface, a significant fraction of these moieties cannot be quenched by I^-(aq). In a simple spherical model for the core one would anticipate that the fraction of accessible chromphores would scale like the area/volume $\sim 1/R_c$. While this is approximately what is observed, we do not have a method at hand to differentiate a "solid core" model, similar to what is expected for diblock polymer micelles and a "microporous core" and similar to classical latexes according to the studies of Winnik et al.[35] and the probable structure of "photoszymes" studied by Guillet et al.[36]

Acknowledgment. TEM measurements were performed by John Mendenhahl at The Cell Research Institute at the University of Texas at Austin. This research was supported by the National Science Foundation Polymers Program (Grant DMR-93-08307). We would like to acknowledge helpful comments by Professor P. Munk of this Department.

References and Notes

(1) Ceresa, R. J. *Block and Graft Copolymers*; Butterworths: London, 1962.
(2) Battaerd, Hai; Tregear, G. W. *Graft Copolymers*; Wiley: New York, 1967.
(3) Molau, G. E. *Colloidal and Morphological Behavior of Block and Graft Copolymers*; Plenum Press: New York, 1971.
(4) Frere, Y.; Gramain, P. *Makromol. Chem.* **1987**, *188*, 593.
(5) Tuzar, Z.; Kratcohvil, P.; Prochazka, K.; Contractor, K.; Hadjichristidis, N. *Makromol. Chem.* **1989**, *190*, 2967.
(6) (a) Watanabe, A.; Matsuda, M. *Macromolecules* **1985**, *18*, 273. (b) Watanabe, A.; Matsuda, M. *Macromolecules* **1986**, *19*, 2253.

(7) Kim, J. H.; Keskkula, H.; Paul, D. R. *J. Appl. Polym. Sci.* **1990**, *49*, 183.
(8) Balazs, A. C.; Pan, T. *Langmuir* **1993**, *9*, 3402.
(9) Xu, R.; Winnik, M.; Riess, G.; Chu, B.; Croucher, M. D. *Macromolecules* **1992**, *25*, 644.
(10) Riess, G.; Calderara, F.; Hruska, Z.; Hurtrez, G.; Lerch, J.-P.; Nugay, T. *Macromolecules* **1994**, *27*, 1210.
(11) Weiss, P.; Gerecht, J.; Krems, J. *J. Polym. Sci.* **1959**, *35*, 343.
(12) (a) Qui, Y.; Yu, X.; Feng, L.; Yang, S. *Makromol. Chem.* **1992**, *193*, 1377. (b) Qui, Y.; Yu, X.; Feng, L.; Yang, S. *Chin. J. Polym. Sci.* **1993**, *11*, 67.
(13) Ramasami, T.; Bhaska, G.; Mandal, A. B. *Macromolecules* **1993**, *26*, 4083.
(14) Barany, G.; Zalipsky, S.; Chang, J. L.; Albericio, F. *React. Polym.* **1994**, *22*, 243.
(15) (a) Berlinova, I. V.; Amzil, A.; Tsvetkova, S.; Panayotov, I. M. *J. Polym. Sci., Part A* **1994**, *32*, 1523. (b) Berlinova, I. V.; Amzil, A.; Panayotov, I. M. *J. Mater. Sci.-Pure Appl. Chem.* **1992**, *a29*, 975. (c) Berlinova, I. V.; Panayotov, I. M. *Makromol. Chem.* **1992**, *190*, 1515.
(16) (a) Wesslen, B.; Friej-Larsson, C.; Kober, M.; Ljungh, A.; Pauisson, M.; Tengvall, P. *Mater. Sci. Eng.* **1994**, *c1*, 127. (b) Wesslen, B.; Jannasch, P. *J. Polym. Sci., Part A* **1993**, *32*, 1519. (c) Wesslen, K. B.; Wesslen, B.; Bo, G. *J. Polym. Sci., Part A* **1992**, *30*, 1799. (d) Wesslen, K. B.; Wesslen, B. *J. Polym. Sci., Part A* **1992**, *30*, 355. (e) Wesslen, B.; Derand, H. *J. Polym. Sci., Part A* **1995**, *33*, 571.
(17) *The Sadtler Standard Spectra*; Ultraviolet Spectra; Sadtler Research Laboratories: Philadelphia, PA, 1968.
(18) (a) Procházka, K.; Kiserow, D.; Ramireddy, C.; Tuzar, Z.; Munk, P.; Webber, S. E. *Macromolecules* **1992**, *25*, 454. (b) Chan, J.; Fox, S.; Kiserow, D.; Ramireddy, C.; Munk, P.; Webber, S. E. *Macromolecules* **1993**, *26*, 7016.
(19) Brandrup, J.; Immergut, E. H. *Polymer Handbook*; John Wiley and Sons: New York, 1989; Vol. VII, p 409.
(20) Lakowicz, J. R. *Principles of Fluorescence Spectroscopy*; Plenum Press: New York, 1983; p 280.
(21) (a) Demas, J. N. *Excited State Lifetime Measurements*; Academic Press: New York, 1983. (b) O'Connor, D. V.; Phillips, D. *Time-correlated Single Photon Counting*; Academic Press: Orlando FL, 1984. (c) Press, William, H. *Numerical Recipes in C*; Cambridge University Press: New York, 1988.
(22) Assuming the densities of the micelles are constant, this corresponds to $(d_{TEM})_w = \sum d_i^2/\sum d_i$ where the summation extends over all the micelles in the sample.
(23) Kiserow, D.; Chan, J.; Ramireddy, C.; Munk, P.; Webber, S. E. *Macromolecules* **1992**, *25*, 5338.
(24) (a) Morishima, Y.; Kobayashi, T.; Nozakura S-I.; Webber, S. E. *Macromolecules* **1987**, *20*, 807. (b) Morishima, Y.; Lim, H. S.; Nozakura, S-I.; Sturtevant, J. L. *Macromolecules* **1989**, *22*, 1148.
(25) Morishima, Y.; Tominaga, Y.; Nomura, S.; Kamachi, M. *Macromolecules* **1992**, *25*, 861.
(26) From: Berlman, I. B. *Energy Transfer Parameters of Aromatic Compounds*; Academic Press: New York, 1973. R_0^{NN} = 11 Å for naphthalene self-transfer. In ref 25 R_0 is estimated to be 8.3 Å.
(27) (a) Myers, J. D.; Friedrichs, M.; Friesner, R. A.; Webber, S. E. *Macromolecules* **1988**, *21*, 3402. (b) Byers, J. D.; Friedrichs, M.; Friesner, R. A.; Webber, S. E. In *Molecular Dynamics in Restricted Geometries*; Klafter, J., Drake, J. M., Eds.; John Wiley and Sons, Inc.: New York, 1989); p 99. (c) Byers, J. D.; Parsons, W. S.; Friesner, R. A.; Webber, S. E. *Macromolecules* **1990**, *23*, 4835. (d) Byers, J. D.; Parsons, W. S.; Webber, S. E. *Macromolecules* **1992**, *25*, 5935.
(28) Eckert, A. R.; Hsiao, J.-S.; Webber, S. E. *J. Phys. Chem.* **1994**, *98*, 12025.
(29) *CRC Handbook of Chemistry and Physics*, 66th ed.; CRC Press, Inc.: Boca Raton, FL, 1986.
(30) This was pointed out to us by Prof. Petr Munk of this Department.
(31) (a) de Gennes, P.-G. *Adv. Colloid Interface Sci.* **1987**, *278*, 189. (b) de Gennes, P.-G. *Macromolecules* **1980**, *13*, 1069.
(32) Halperin, A. *Macromolecules* **1987**, *20*, 2943.
(33) We note that in the data on polystyrene−PEO diblock polymer micelles presented by Xu et al. (ref 9, Table IV) that S_{PEO} obeys a much stronger N_B dependence, i.e. $S_{PEO} \propto N_B^{0.393}$, than predicted by the Halperin model.
(34) Since the UV−vis and NMR differ by essentially a constant factor, the slope is similar for all data in these tables.
(35) (a) Pekcan, Ö.; Egan, L. S.; Winnik, M. A.; Croucher, M. D. *Macromolecules* **1990**, 423, 2210. (b) Winnik, M. A.; Disanayaka, B.; Pekcan, Ö.; Croucher, M. D. *J. Colloid Interface Sci.* **1990**, *139*, 251.
(36) See: Nowakowska, M.; Guillet, J. E. *Macromolecules* **1991**, *24*, 474 and references therein to earlier work.

MA951053H